

Elucidation of specific ion association in nonaqueous solution environments*

Masashi Hojo[‡]

Faculty of Science, Kochi University, Akebono-cho, Kochi 780-8520, Japan

Abstract: The paper reviews ion aggregation in ionic solution in solvents of low and high permittivity. Although higher ion aggregates from 1:1 type electrolytes in low-permittivity media ($\epsilon_r < 10$) are widely accepted, only a few chemists have recognized the higher ion aggregation in the higher-permittivity media. However, we have clarified that the chemical interaction, such as coordination, can operate between simple anions and cations in nonaqueous solvents ($20 < \epsilon_r < 65$) of low solvation ability. Acids (HA) and their conjugate base anions (A^-) may react with each other to form homoconjugated species, such as $A^-(HA)_2$, in acetonitrile or benzonitrile (i.e., solvents possessing poor hydrogen-bonding donor and acceptor abilities). An analytical method of conductivity data for 1:1 electrolytes has been developed and successfully applied to very complicated systems, in which the ion pair (1:1), triple ions (2:1 and 1:2), and the quadrupole (2:2 association) are involved in a solution at the same time. After observing the direct reaction of some anions (e.g., Cl^-) and cations (e.g., Li^+) toward a certain species, we interpreted comprehensively the salt effects in chemical equilibria, based on distinct chemical interactions and not merely a vague term, “medium effect”. The mechanism of salt effects on solvolysis reactions of the S_N1 type in organic–aqueous mixed solvents has been elucidated. We discussed that a reaction manner similar to that in nonaqueous solution can take place even in some “aqueous” solution if the huge network of hydrogen-bonding of bulk water (the number of water, $n_w > \sim 10^8$) is destroyed due to any spatial barriers (such as ions, molecules, surface) or elevated temperature.

Keywords: nonaqueous solvent; acetonitrile; ion pair formation in higher-permittivity media; water structure by hydrogen bonding; property of bulk water; activity coefficient.

INTRODUCTION

In aqueous solution, alkali metal and alkaline earth metal ions of relatively low concentrations are often regarded as supporting electrolytes or “indifferent” salts. The effects of indifferent salts can be evaluated by the Debye–Hückel theory. However, at more than ca. 0.1 mol dm^{-3} of 1:1-type strong electrolytes, the assumption or approximation in the theory becomes no more valid; and at the same time, specific interaction between solutes can play a role in the reaction. With additional empirical terms, the theory can be extended to higher concentration systems. It may be natural that a theory which premises complete dissociation should not be useful because even strong electrolytes do associate at more than ca. 0.1 mol dm^{-3} .

*Paper based on a presentation at the International Conference on Modern Physical Chemistry for Advanced Materials (MPC '07), 26–30 June 2007, Kharkiv, Ukraine. Other presentations are published in this issue, pp. 1365–1630.

[‡]E-mail: mhojo@cc.kochi-u.ac.jp

So far, we have studied the interaction between ions in solution, discovering the fact that the chemical interaction could operate, such as hydrogen bonding or coordination, as well as Coulombic interaction between alkali metal or alkaline earth metal ions and anions (excluding ClO_4^- , etc.) in poor solvating solvents, especially in a hydrophobic aprotic solvent. A hydrophobic aprotic solvent has weak accepting and donating abilities in hydrogen-bonding interaction with solutes. However, a huge number of studies have been performed without taking into account the “minor” interaction between alkali metal ions and anionic or uncharged species. For instance, solvent effects have been examined extensively on the protolytic equilibria of many dye compounds following the orthodox or conventional procedure [1].

In the present paper, a number of specific chemical reactions mainly in protophobic aprotic solvents are examined from the viewpoint of the ion association between or among ions and molecules as well as the changes in activity coefficients of ions. Remarkable deviation from the theory based on the complete dissociation of electrolytes has often been observed in a nonaqueous solvent, organic solvent mixed aqueous solution, and even aqueous solution containing concentrated salts; abnormal deviation may also appear in chemical equilibria or reaction rates of two-phase separation methods, such as solvent extraction and high-performance liquid chromatography (HPLC). The reason why specific reactions often occur in such conditions will be discussed.

SPECIFIC INTERACTIONS BETWEEN SOLUTES IN NONAQUEOUS SOLUTION

Assessment of residual water in nonaqueous solvents

Nonaqueous solvents, such as acetonitrile, contain essentially small amounts of water (several mM) even after drying of solvents. Therefore, many chemists may suspect that the property of a solvent for the common use differs much from that of the “absolutely dried solvent”. Coetzee and Kolthoff [2] prepared an anhydrous perchloric acid in acetic acid by heating a solution of 71 % aqueous perchloric acid in glacial acetic acid with the amount of acetic anhydride required to remove the water present; this stock solution was diluted by acetonitrile to give an anhydrous perchloric acid-acetonitrile solution for the base titration. However, the acetic acid in the solution may interfere with certain reactions. Kinugasa et al. [3] prepared anhydrous perchloric acid by the distillation method in order to examine the interaction between CH_3CN and HClO_4 . The water contents in nonaqueous solvents are determined by means of the Karl-Fisher method or gas chromatography equipped with a column of “Porapak Q” [4].

It may be reasonable to regard that the water of small amounts (residual water) in nonaqueous solvents causes no remarkable effects on the chemical equilibria or reaction rates of the solutes in the solvents; the reason will be shown as follows. The bulk water is highly structured through the hydrogen-bonding network. The common water properties should come from the bulk water of a huge number. The bulk water plays as a rather “strong” acid and also “strong” base. However, isolated water molecules are expected to give some properties much different from the bulk water because the isolated water molecules have no interaction with other water molecules or no help by other water molecules. Considering the fact that higher aggregation of water molecule can take place even in the vapor phase [5], an absolutely isolated water molecule could be achieved just in the vapor phase with a low density at a higher temperature.

As for the acidity or basicity, we cannot find any large difference between “isolated” water (H_2O) and diethyl ether (Et_2O) or methanol (MeOH): for instance, the donor number of water [6], which is dispersed in dichloroethane, has been evaluated to be 18; this value is very close to that of diethyl ether or methanol. According to Gutmann [6], “it is noteworthy that even water, which has unusual entropic effects as a bulk solvent, fits the linear relationship with other solvents when the water is present in a diluted solution of dichloroethane.” The intrinsic acidity of the single water molecule without hydrogen bonding is extremely smaller than expected from the bulk water: the O–H bond of a water molecule

cannot be broken easily because the enthalpy of the bond has been evaluated to be 463 kJ mol^{-1} for each bond; the value is larger than that (413 kJ mol^{-1}) of a C–H bond in methane [7].

Figure 1 shows the chemical shift values (vs. TMS) we observed of H_2O proton NMR with changing water contents in acetonitrile (MeCN). The “residual” water in dried acetonitrile gave a chemical shift value of ca. 2.1, however, with increasing content of water, the value increased and approached that of bulk water (ca. 4.7). Alcohols such as methanol, ethanol, and others, possessing a hydrogen-bonding structure, also showed similar behavior in their chemical shifts. Silverstein et al. [8] noted the difference between the bulk water and the isolated water as follows: the chemical shift of the bulk water, i.e., the film of water on the wall of the NMR tube which contains CDCl_3 or suspended water in CDCl_3 appears at $\delta = \text{ca. } 4.7$, while the “monomeric” dissolved water in CDCl_3 at $\delta = 1.5$, which should disturb the important signals of organic compounds. The residual water or a small amount of water in propylene carbonate (PC) [9], acetone, and dimethyl sulfoxide (DMSO) [10] has been reported to give a smaller chemical shift value.

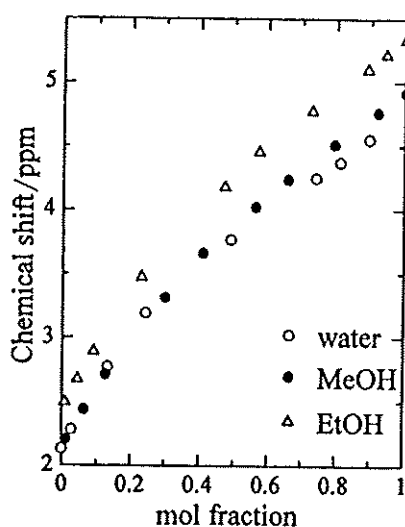


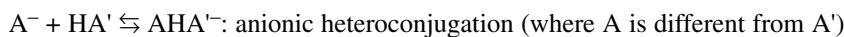
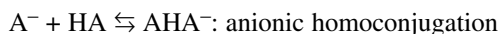
Fig. 1 The changes of OH-proton chemical shift values for water, methanol, and ethanol in CD_3CN .

As described above, the acidity and basicity of the residual water in a nonaqueous solvent should be extremely small because the water cannot form huge networks of water molecules; in other words, the effects on solutes of water at a sufficiently low concentration in a nonaqueous solvent must be no more than those of diethyl ether. However, strong Lewis acids, such as Al^{3+} or In^{3+} , may react with “isolated” water molecules. Therefore, it goes without saying that, for the studies of nonaqueous solutions, great care should be taken with the drying of solvents, glassware, and reagents and even the effects of moisture in the atmosphere. In laboratories operating nonaqueous solvents, it is a daily procedure to remove the surface water on glassware in a drying oven at 120°C . The hysteresis of glass on heating of flasks should always be taken into account.

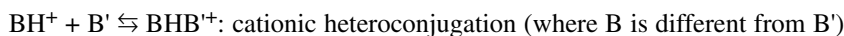
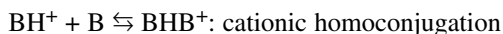
Homo- and heteroconjugation

In amphiprotic solvents, such as water and ethanol, the interaction between solvents and solutes is strong enough to prevent the solutes from interacting together through the hydrogen-bonding interaction. However, in aprotic solvents, the conjugate anions (A^-) from weak acids (HA) may interact with

the mother acid or a related acid (HA') molecule to form anionic homo- or heteroconjugated species as follows:



Similarly, cationic homo- or hetero-conjugated species are derived from the interaction between a weak base (B) and the conjugate acid (BH⁺):



By means of conductometry, we [11] discovered that even sulfonic acids, such as methanesulfonic and *p*-toluenesulfonic acids, behave indeed as weak acids in benzonitrile ($\epsilon_r = 25.2$) to form 1:2-type homoconjugated species, A⁻(HA)₂ (cf. Fig. 2). Benzonitrile has rather small values of donor and acceptor numbers, DN = 11.9 and AN = 15.5. Coincidentally, Kolthoff and Chantooni [12] observed a distinct maximum at the 2/3 equivalent point in the conductometric titration of H₂SO₄ with butylamine; they attributed the appearance of the maximum to the formation of 1:1-type homoconjugated species (HSO₄⁻·H₂SO₄). However, we have argued that the appearance of the maximum at the 2/3 equivalent point should be based on a 2:1-type homoconjugated species (Scheme 1) and not the 1:1-type one [11].

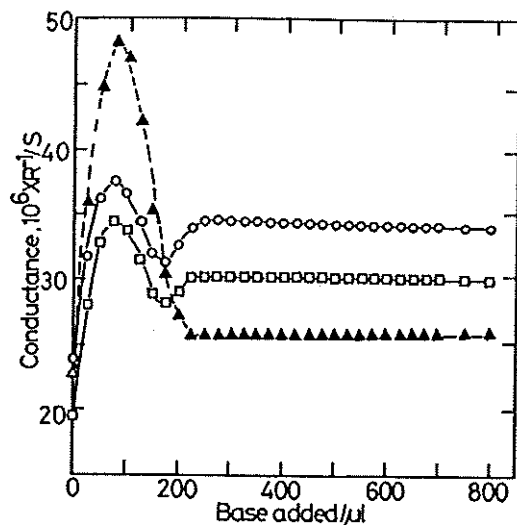
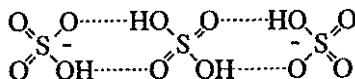
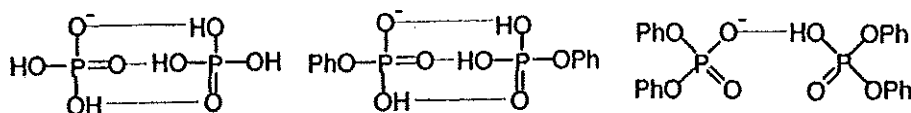


Fig. 2 Conductometric titration curves of 0.0050 M sulfonic acids (25 ml) with 0.50 M triethylamine in benzonitrile at 25 °C: (▲) methanesulfonic, (□) *p*-toluenesulfonic, (○) benzenesulfonic acids.



Scheme 1 The proposed homoconjugated species, (HSO₄⁻)₂·H₂SO₄.

Phosphoric acids can cause aggregation, including homoconjugation, even in dimethylformamide (DMF) with large donicity ($DN = 26.6$) [13]. It has been demonstrated that the stability of the 1:1-type species depends on the number of OH groups in a phosphoric acid molecule concerning the homoconjugation reaction (cf. Scheme 2).



Scheme 2 Homoconjugation with single and triple bonds between HA and A⁻ in DMF.

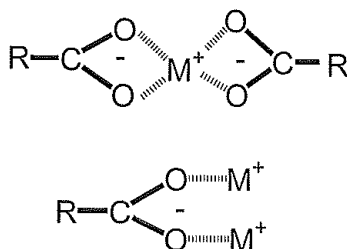
Complex between aza-crown ethers and alkali metal ions

The complex formation abilities of alkali metal ions are much smaller than those of transition-metal ions. In aqueous solution, the weak complexes with alkali metal ions are often neglected, and a strong dependence of protonation constants for ligands on the concentration of background is generally ascribed to activity factors. However, Daniele et al. [14] stressed that a rigorous treatment of acid–base equilibria must also take into account the weak interaction between the ligand under study and the cation background. The complex formation between alkali metal ions and the acetate ion has been examined in aqueous solutions at different temperatures and ionic strengths [15]. The complex formations of alkali metal ions with macrocyclic compounds, such as crown ethers, have been investigated widely by means of various techniques [16].

In MeCN, aza-crown ethers give anodic (mercury-dissolution) waves of polarography; the half-wave potential ($E_{1/2}$) of the anodic waves are shifted by the addition of Lewis acids, such as alkali metal ions. The shifts in $E_{1/2}$ have been utilized to evaluate the complex formation constants between aza-crown ethers and alkali metal ions in MeCN [17–19]. In a similar method, the interaction between acyclic polyamines and alkali metal ions has been also evaluated [20].

Coordination and “reverse-coordination”

By means of a usual polarographic method, we [21] have discovered the 1:2-type complexes of Li⁺, Na⁺, and K⁺ with the benzoate ion in MeCN (cf. Scheme 3), evaluating the overall formation constants (K_f/M^{-2}) to be $10^{16.7}$, $10^{8.4}$, and $10^{4.2}$, respectively, in the presence of a large excess of PhCOO⁻(Et₄N⁺). The cathodic wave of Li⁺(ClO₄⁻) shifts negatively with the addition of Cl⁻(Et₄N⁺): the formation constants of Li⁺(Cl⁻)_{*n*} (*n* = 1–4) have been obtained [22].



Scheme 3 The coordination and “reverse-coordination” for alkali metal ions.

On the other hand, the formation of a “reverse-coordinated” species, $\text{RCOO}^-(\text{M}^+)_2$, has been proposed on the base of the redissolution of RCOO^-M^+ ($\text{M}^+ = \text{Li}^+$ or Na^+) by the addition of a large excess of LiClO_4 or NaClO_4 in MeCN [21]; where “reverse-coordination” represents a reaction of two metal ions toward a single charged anion, which is completely different from “back donation” [cf., 23]. Murray [24] and Itabashi [25] have suggested the formation of “reverse-coordinated” species for acetylacetonate and acetate ions, respectively.

UV–vis spectroscopy verified the formation of “reverse-coordination” for carboxylate ions [26]. Figure 3 shows the change in absorbance at ca. 225 nm of PhCOO^- with increasing concentration of LiClO_4 or NaClO_4 . The absorbance decreased in the presence of an equivalent-amount metal ion, forming white precipitates, however, it increased in the presence of large amounts of the metal ion with redissolution of the precipitates. We note that the precipitates were never dissolved by the addition of a large excess of Et_4NClO_4 . Apart from the change of solubility, the “reverse-coordination” was caught in the spectral changes of 2,4-dinitrobenzoate ion (cf. Figs. 4a and 4b); the addition of LiClO_4 up to the equivalent amount of the benzoate ion caused the decrease in the absorbance around 300 nm and, at the same time, the increase around 250 nm without precipitation; the appearance of an isosbestic point at 297 nm indicates the presence of A^- and Li^+A^- . The isosbestic point was shifted from 297 to 291 nm by the addition of an excess of Li^+ , which may suggest the coexistence of Li^+A^- and $(\text{Li}^+)_2\text{A}^-$. In benzonitrile [26], a similar shift of the isosbestic point was observed for the picrate ion by the addition of Li^+ ; the “reverse-coordination” in addition to the ion pair between Li^+ and the picrate ion was verified in this way.

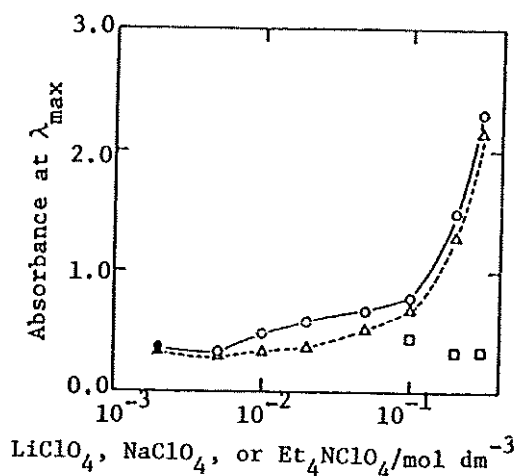


Fig. 3 The absorbance change of the benzoate ion (2.0×10^{-3} M $\text{C}_6\text{H}_5\text{COOEt}_4\text{N}$) by the addition of an excess of LiClO_4 (\circ), NaClO_4 (\triangle), and Et_4NClO_4 (\square , containing 2.0×10^{-3} M LiClO_4). Solid marks show the equivalent amount.

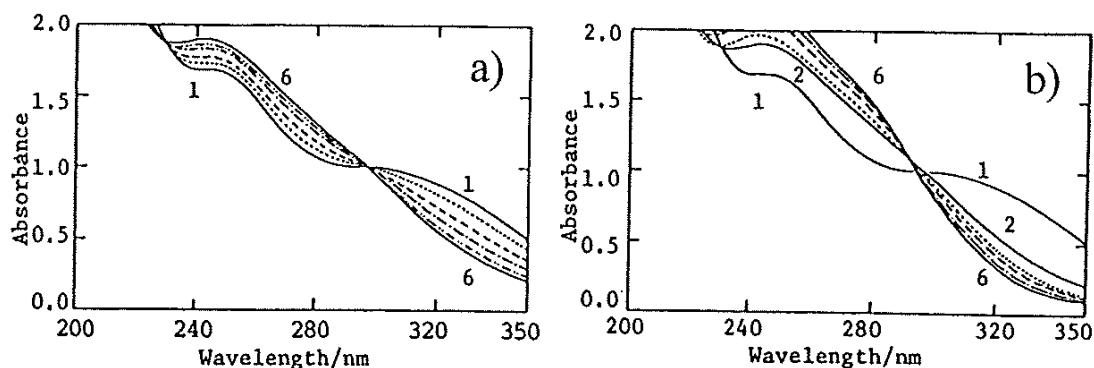


Fig. 4 (a) UV spectral changes with the molar ratio (up to 1:1) of LiClO_4 to 2,4-dinitrobenzoate ion (2.0×10^{-4} M) in MeCN: (solid line 1) 0; (dotted line) 0.2; (broken line) 0.4; (solid line, single dot, solid line) 0.6; (solid line, double dot, solid line) 0.8; (solid line 6) 1.0. (b) UV spectral changes of 2,4-dinitrobenzoate (2.0×10^{-4} M) by the addition of excess amounts of LiClO_4 : (solid line 1) 0; (solid line 2) 2.0×10^{-4} ; (dotted line) 1.0×10^{-3} ; (broken line) 1.0×10^{-2} ; (solid line, single dot, solid line) 4.0×10^{-2} ; (solid line 6) 0.1 and 0.2 M LiClO_4 .

As for the benzenesulfonate ion in MeCN, an excess amount of Li^+ caused the increase in the absorbance as the second Li^+ ion can attack the ion pair to form the “reverse-coordinated” species, whereas the addition of Na^+ caused a monotonous decrease of the absorbance (cf. Fig. 5) [23]. In acetone, the “reverse-coordination” formation constant was evaluated for $(\text{PhO})_2\text{PO}_2^-$ with Li^+ [23]. As described above, a variety of anions, carboxylate, sulfonate, phosphate, and chloride ions, can form certainly 1:2- and 2:1-type complexes in addition to the ion pair with Li^+ (or Na^+).

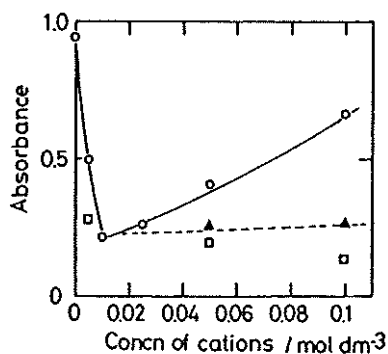


Fig. 5 Changes of absorbance of $\text{Et}_4\text{N}^+\text{C}_6\text{H}_5\text{SO}_3^-$ (5.3×10^{-3} M) with increasing concentration of alkali metal perchlorates in MeCN: (○) LiClO_4 ; (△) NaClO_4 ; (▲) Et_4NClO_4 in addition to 0.01 M LiClO_4 .

Now, we may consider the role of the perchlorate ion, ClO_4^- . The perchlorate ion can be regarded to have almost no complex formation ability because of its excellent three-dimensional symmetry. Similarly, BF_4^- , PF_6^- , and tetraalkylammonium ions (such as Et_4N^+) in solution may cause no chemical interactions through coordination or hydrogen bonding since the coordination numbers of the central elements in the species (ions) are fully satisfied, apart from their excellent three-dimensional symmetries. A possible coordination between transition-metal ions and the perchlorate ion has been suspected [28], however, the interaction is not clearly demonstrated.

Hickey et al. [29] reported a certain “leveling effect”, that the polarographic reduction potentials of carboxylic acids in pyridine solution approached those of strong acids, such as perchloric and

p-toluenesulfonic acids, with the addition of Li^+ . We have succeeded in explaining the “leveling effect” quantitatively, on the base of the formation of the free pyridinium ion (PyH^+), formed through the $\text{RCOO}^-(\text{Li}^+)_2$ species [30], while Tsuji and Elving [31] tried to explain the phenomena by the ion association and ion-exchange reactions.

CONDUCTOMETRY IN NONAQUEOUS AND AQUEOUS SOLUTIONS

Ion pairs and higher ion aggregates by conductometry

The conditions and concentrations of chemical species can be examined by conductometry, based on the transformation phenomena of ionic species. In usual theories or analyzing methods of conductometry, it is premised that electrolytes in solution dissociate completely or associate partly and no higher association above the ion pair formation takes place. This premise must be valid in dilute aqueous solutions, however, higher ion aggregation in addition to the 1:1-type ion pair formation may occur in conditions of lower permittivities, lower solvation abilities, higher ion concentrations, and so on. Applying a conductometric theory to a system including the ion pair and the higher ion aggregate together should cause distortion, even if the theory is much sophisticated; and the analysis may result in a complete failure.

Triple-ion formation in low-permittivity media

As early as 1933, Fuoss and Kraus [32] proposed that the Coulombic interaction between the ion pair (M^+X^-) and the ion (M^+ or X^-) can operate to form “symmetrical” triple ions (M_2X^+ and MX_2^-) in low-permittivity media ($\epsilon_r < 23.2$). The minima observed in conductometric curves ($\Lambda - C^{1/2}$) in very low permittivity media ($\epsilon_r < 10$) were interpreted by the formation of this kind of species. Although the cause of appearance of the minimum may sometimes be attributed to other factors [33,34] and not the triple-ion formation, the higher ion aggregates in low-permittivity media are widely accepted.

A linearity was demonstrated, for the first time [35], between the salt concentrations at which the minima appear and the triple-ion formation constants in low-permittivity media, such as tetrahydrofuran (THF, cf. Fig. 6) and 1,2-dimethoxyethane. This linearity was predicted long ago [36]. The reason why the prediction has not been demonstrated for a long time may be as follows: in low-permittivity media, some of the very common electrolytes, such as lithium chloride, do not give minima in the conductometric curves because of remarkable dimerization of the ion pairs [35]. Figure 7 shows the changes in the equilibrium concentrations of the single ions, the ion pairs, and the triple ions from lithium picrate, which hardly forms the quadrupole (the dimer of ion pairs).

Lithium bromide, differing from LiCl, gave a minimum ($C_{\text{min}} = 4.9 \times 10^{-3} \text{ mol dm}^{-3}$) in THF. The molar conductivities at different salt concentrations were explained by the formation of the ion pair and “symmetrical” triple ions, accompanying the quadrupole formation at a moderate level. Interestingly, the C_{min} was increased by the addition of a small amount of 2-ethyl-1-hexanol to the THF solution, though the permittivities of the alcohol and THF are reported to be the same ($\epsilon_r = 7.58$). Even at a constant permittivity, the triple ion should become more difficult to form because of the higher solvation by the added protic solvent [37].

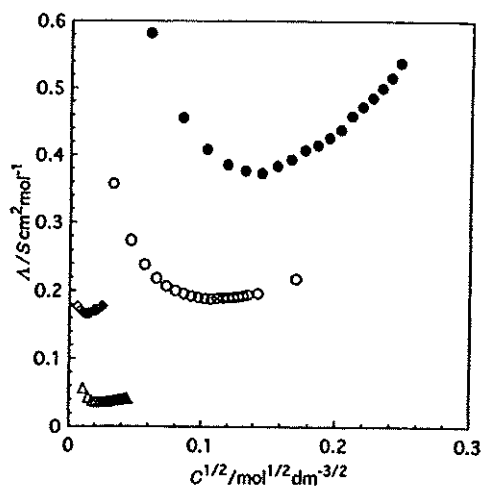


Fig. 6 Observed molar conductivities (Λ) in THF at 25 °C: (●) LiClO_4 ; (○) LiPic; (◇) $2,4\text{-(NO}_2)_2\text{C}_{10}\text{H}_5\text{OLi}$; (△) LiNO_3 .

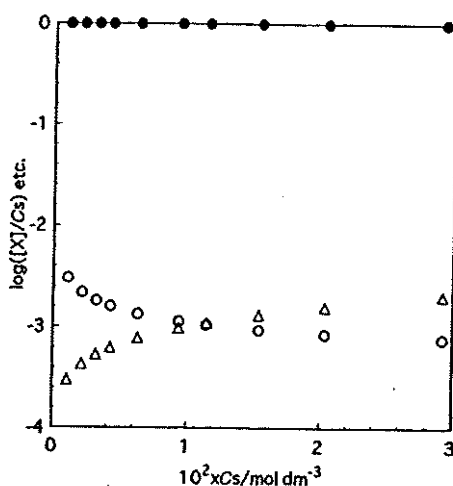


Fig. 7 Changes of equilibrium concentrations of each species with the LiPic concentration in THF: (○) simple ions; (●) the ion pair; (△) triple ions.

Higher ion aggregation in higher-permittivity media

Even with higher permittivities ($20 < \epsilon_r < 65$), in solvents of low solvating abilities, especially in protophobic aprotic solvents, the triple-ion and quadrupole formation from trialkylammonium halides, $\text{R}_3\text{NH}^+\text{X}^-$ [38], and lithium trifluoroacetate [39] can occur through hydrogen bonding and coordination bond forces, respectively, between or among the cation and the anion. For such systems with higher ion aggregates, an analytical method, such as the Shedlovsky analysis [40], in which only 1:1 association is taken into account, should be no longer valid; a typical instance is shown as follows: Figure 8 illustrates the conductometric curve of lithium trifluoroacetate (LiCF_3CO_2) in PC. The molar conductivities (Λ_{calc}), calculated considering only the ion pair formation, fit the observed ones (Λ_{obsd}) at lower salt concentrations (e.g., $4 \times 10^{-4} \text{ mol dm}^{-3}$ and so on), however, they exceed the observed ones at higher concentrations. The formation of the dimer in addition to the ion pair at higher salt concentrations can

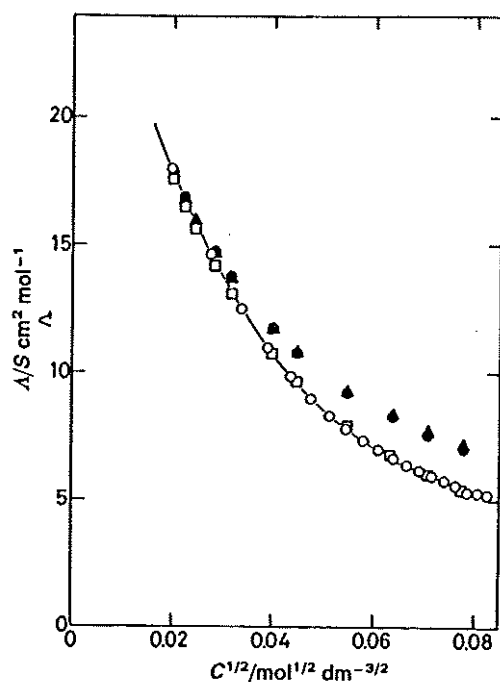


Fig. 8 Observed and calculated Λ values of lithium trifluoroacetate $[(0.4\text{--}6.0) \times 10^{-3} \text{ M}]$ in PC: (\circ) observed; (\bullet) calculated with only ion-pair formation: (\blacktriangle) calculated with ion-pair and (weak) triple-ion formation: (\square) calculated with ion-pair, (weak) triple-ion, and (strong) quadrupole formation.

be the cause of the distortion that Λ_{obsd} values deviated much lower than the expected Λ_{calc} ones. Wu and Friedman [41] failed in analyzing the conductivities of lithium trifluoroacetate in PC, and suggested the formation of the dimer, $\text{Li}_2(\text{CF}_3\text{CO}_2)_2$, based on calorimetric experiments. Later, Jansen and Yeager [42] reported precise conductivity data for the same system, analyzing with the Fuoss–Hisa equation to end in failure, and finally have concluded that the salt forms a variety of species in the solution.

Figure 9 shows the Shedlovsky plots of lithium pentafluoropropionate ($\text{LiC}_2\text{H}_5\text{CO}_2$) in PC: the relation between $1/\Lambda S$ and $CASf^2$ gave not a linear but a concave curve. This system contains remarkable formation of the quadrupole (the dimer of ion pairs) in addition to the ion pair formation at higher salt concentrations. The least-squares method of the concave curve resulted in a much larger limiting molar conductivity (an apparent Λ_0 of 44.86) value than the intrinsic Λ_0 value (24.03): the Kohlrausch additivity law with “strong” electrolytes gave the $\Lambda_0(\text{LiC}_2\text{F}_5\text{CO}_2)$ value; where LiClO_4 , $\text{Et}_4\text{NC}_2\text{F}_5\text{CO}_2$, and Et_4NClO_4 for the Kohlrausch additivity law are all strong electrolytes, or they form the ion pairs weakly at most. We notice that the cation of Et_4N^+ and not a metal ion can make a strong electrolyte, regardless of the kind of anions; similarly, the anion of ClO_4^- makes a strong electrolyte even if the counter cation is a metal ion.

When a strong triple formation occurs in addition to the ion pair, to the contrary, the relation between $1/\Lambda S$ and $CASf^2$ gives a convex curve; the fact that the slope becomes smaller with increasing salt concentration results in a smaller association constant (an apparent K_a). In an extreme case, the slope value is degenerated to zero, that is, $K_a = 0$ (cf. Fig. 10) although strong formation of the ion pair occurs in the real system.

The most curious finding is that the strong electrolyte, LiCF_3CO_2 or $\text{LiC}_2\text{F}_5\text{CO}_2$, in aqueous solution ($\epsilon_r \sim 80$) undergoes a drastic transfiguration into a very weak electrolyte in PC ($\epsilon_r \sim 65$). Barthel et al. [43] have criticized this point; and they also denied the formation of quadrupole (2:2 association) in the analysis of their conductivity data. Now, a change in conception may be needed to understand the

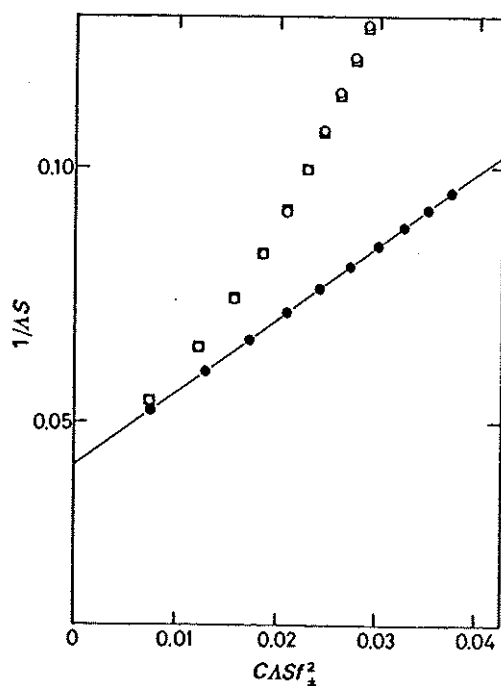


Fig. 9 Shedlovsky plots for $\text{LiC}_2\text{F}_5\text{CO}_2$ in PC: (○) experimentally observed points; (□) simulated points with ion-pair, triple-ion, and quadrupole formation; (●) simulated points with ion-pair formation.

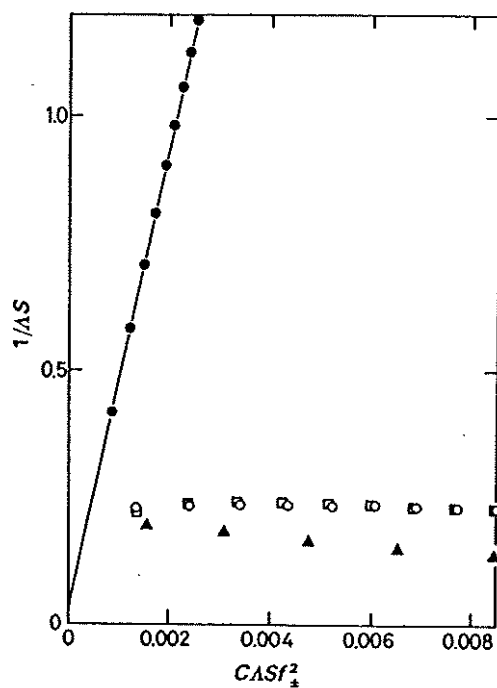


Fig. 10 Shedlovsky plots for $\text{LiC}_2\text{F}_5\text{CO}_2$ in PhCN: (○) experimentally observed points; (□) simulated points with ion-pair, triple-ion, and quadrupole formation; (▲) simulated points with ion-pair and triple-ion formation; (●) simulated points with ion-pair formation.

phenomena as follows: Li^+ and CF_3CO_2^- (or $\text{C}_2\text{F}_5\text{CO}_2^-$) cannot fulfill the required conditions to be a component of strong electrolytes any more in PC, a protophobic aprotic solvent, and they may behave as if H^+ and CH_3COO^- , respectively, are in aqueous solution.

In acetonitrile, Li^+PMBP^- (lithium 1-phenyl-3-methyl-4-benzoyl-5-pyrazolonate: a kind of β -diketonate) gave a minimum on the conductivity curve; the molar conductivities were explained by higher ion association including the triple-ion formation (Fig. 11) [44]. The triple ions consist of two types of ions, $\text{Li}^+(\text{L}^-)_2$ and $(\text{Li}^+)_2\text{L}^-$. A calculation has demonstrated that the minimum never appears without both types of triple ions of good amounts at the same time. The formations of the tetra-coordinated species, $\text{Li}^+(\text{L}^-)_2$, and the reverse-coordinated species, $(\text{Li}^+)_2\text{L}^-$, were confirmed by means of ^7Li NMR and UV-vis absorption spectroscopy, respectively.

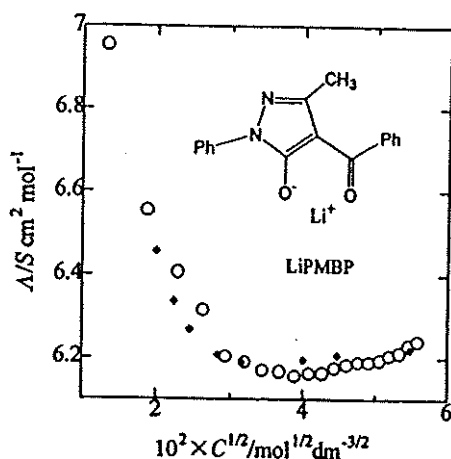


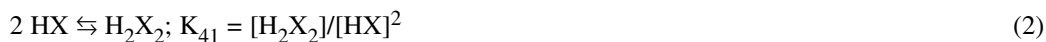
Fig. 11 $\Lambda - C^{1/2}$ plots of lithium 1-phenyl-3-methyl-4-benzoyl-5-pyrazolonate (LiPMBP) in MeCN at 25 °C: (○) observed; (◆) calculated with ion-pair, triple-ion, and quadrupole formation.

Dimerization of acetic acid molecules in aqueous solution

It is well known that carboxylic acids, such as acetic acid, dimerize through the hydrogen-bonding force in nonpolar solvents, benzene and carbon tetrachloride. Whereas, in aqueous solution of diluted acetic acid, the acid molecules should dissociate to be acetate ions, and the interaction between the solute and water through hydrogen bonding should be strong; therefore, no dimerization of acetic acid takes place. However, it has been suggested that acetic acid of higher concentrations, such as cryoscopic data, Raman spectra, vapor pressure measurements, and other various methods [45]. Suzuki et al. [46] reported the pressure effects on the dimerization of carboxylic acids in aqueous solution. In conductometric studies of slightly higher concentrations at which the Debye-Hückel theory should still hold, the calculated thermodynamic ionization constants have shown pronounced deviations from the extrapolated value; these deviation were attributed to the "medium effects" of the nonionized acetic acid molecules on the ionization of the acid. Analyzing conductivity data strictly, however, Katchalsky et al. [47] has insisted that the deviation of the dissociation constant is based on the dimerization of acetic acid molecules.

In the present study, using our analytical method, we carried out the analysis of the data that Katchalsky et al. analyzed [48]. We would like to clarify the mechanism that some distortion occurs on the analysis of conductivity data of the electrolytes with the progress of dimerization. Our analytical method is outlined as follows: where HX represents acetic acid and the electric charges are omitted.





The total concentration of acetic acid being expressed by C_s , the mass balance for the proton is

$$C_s = [\text{H}] + [\text{HX}] + 2[\text{H}_2\text{X}_2] \quad (3)$$

Equation 4 is derived by introducing eqs. 1 and 2 into eq. 3.

$$2 K_{41} K_1^2 [\text{X}]^4 + K_1 [\text{X}]^2 + [\text{X}] - C_s = 0 \quad (4)$$

The relation is expressed by eq. 5 between the molar conductivity (Λ) and C_s , the equilibrium concentration $[\text{X}]$, and the corrected limiting molar conductivity Λ_0' , as $[\text{H}] = [\text{X}]$.

$$\Lambda = \Lambda_0' [\text{X}]/C_s \quad (5)$$

For the correction of the limiting molar conductivity, Onsager's limiting equation ($\Lambda_0' = \Lambda_0 - (\alpha\Lambda_0 + \beta)\sqrt{I}$) was utilized; where α , β , and I are the terms concerning relaxation and electrophoretic effects and the ionic strength, respectively. The optimal values of K_1 and K_{41} in eq. 4 were searched out by the trial and error method for the every Λ value over the measured concentration range. The activity coefficients of ionic species were corrected by the Debye–Hückel equation.

Table 1 shows the molar conductivities ($\Lambda/S \text{ cm}^2 \text{ mol}^{-1}$) of acetic acid in water observed by MacInnes and Shedlovsky [48]; the relative error in the calculated Λ value by our analytical method is expressed as the % unit. Trying to explain the observed conductivities with only a 1:1 ion pair formation constant, the observed values became distinctly below the calculated ones at more than 0.02 M of the acetic acid concentration; where $K_1 = 5.7045 \times 10^4$, i.e., the inverse value of the dissociation constant adapted by Katchalsky et al. [47] of 1.753×10^{-5} and $\Lambda_0 = 390.59$ were used as they are. When the dimerization constant $K_{41} = 0.17$ was introduced in addition to the ion pair formation, every calculated value fits the observed one within $\pm 0.1\%$ of the relative error for whole concentration range of $2.8 \times 10^{-5} \sim 0.23$ M. By the way, Katchalsky gave 0.16 as the dimerization constant and not 0.17. Figure 12 shows the equilibrium concentrations of the species, the simple ion, the ion pair, and the

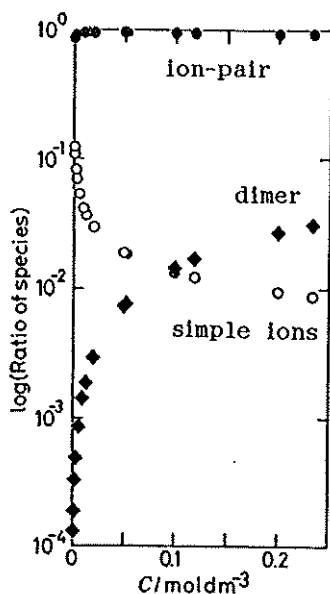


Fig. 12 Changes of equilibrium concentrations of each species with the CH_3COOH concentration in H_2O calculated with $K_1 = 5.7045 \times 10^4$ and $K_{41} = 0.17$: (○) simple ions, $[\text{H}^+] = [\text{CH}_3\text{COO}^-]$; (●) the ion pair, $[\text{CH}_3\text{COOH}]$; (◆) the dimer, $[(\text{CH}_3\text{COOH})_2]$.

dimer, calculated using the ion pair and the dimer formation constants. In the figure, the very lower concentration range is not displayed; the ion pair (the acetic acid molecule) occupied almost all parts of the ratio for the wide concentration range ($1 \times 10^{-3} \text{ M} < C_s < 0.23 \text{ M}$). With increasing acetic acid concentration, the concentration of the dimer ($[\text{H}_2\text{X}_2]$) increases at the expense of the ion pair ($[\text{H}] = [\text{X}]$), and finally the dimer exceeds the simple ion at around 0.1 M.

Table 1 Molar conductivities ($\Lambda/\text{S cm}^2 \text{ mol}^{-1}$) of acetic acid in water at 25 °C observed by MacInnes and Shedlovsky^a and the relative error in the calculated Λ values by our analytical method.

No.	$10^3 \times C^b/\text{M}$	$\Lambda/\text{S cm}^2 \text{ mol}^{-1}$	Rel. error/% ^c	Rel. error/% ^d
1	0.028 014	210.32	+0.01	+0.01
2	0.111 35	127.71	-0.02	-0.03
3	0.153 21	112.02	+0.10	+0.10
4	0.218 44	96.466	+0.05	+0.05
5	1.028 31	48.133	+0.05	+0.03
6	1.363 40	42.215	-0.01	-0.03
7	2.414 00	32.208	+0.05	+0.01
8	3.440 65	27.191	+0.06	+0.01
9	5.911 53	20.956	+0.07	-0.02
10	9.8421	16.367	+0.10	-0.05
11	12.829	14.371	+0.23	+0.03
12	20.000	11.563	+0.33	+0.02
13	50.000	7.356	+0.076	-0.00
14	52.303	7.200	+0.70	-0.10
15	100.00	5.200	+1.49	-0.01
16	119.447	4.759	+1.65	-0.13
17	200.00	3.650	+2.94	+0.06
18	230.785	3.391	+3.30	+0.01

^aRef. [48].

^bThe analytical concentration of acetic acid.

^cCalculated with K_1 alone.

^dCalculated with $K_1 = 5.0745 \times 10^4$ and $K_{41} = 0.17$.

Now that acetic acid forms the dimer (quadrupole) in addition to the ion pair in aqueous solution, any theoretical equation expecting the formation of only 1:1-type ion pair should fail in the analysis, just as lithium trifluoroacetate in PC, even if the theory is highly developed. In principle, the Shedlovsky method has the advantage that it can be applied in almost every case and is not dependent on data of high precision. Analyzing the conductivity data in Table 1 with the Shedlovsky method, the apparent Λ_0 and K_a were deviated as predicted above. Completely different Λ_0 values were given for the data of only very low concentration ranges and those including higher concentration ranges: the apparent Λ_0 values increased remarkably as 391.28, 402.51, 542.69, and 1046.2 for the sampling points of 1–8, 1–12, 1–16, and 1–18, respectively, while the apparent K_a value increased from 5.73×10^4 to 4.24×10^5 .

As the summary of this section, the analyzing method by Katchalsky [47] is useful for a system including the 1:1-type ion pair and the dimer formations. On the other hand, the Fuoss–Kraus method [32] can be applied to a system of triple-ion formation in addition to the ion pair. However, both methods are not intended to apply to a system in which the triple-ion formation and the dimerization of ion pairs proceed at the same time. Our analytical method [23,37,39,44], generalized by adding the term of the triple-ion formation to eq. 4, is completely different from their methods, and can be utilized for any systems in which the 1:1-type ion association, the triple-ion formation, and the dimerization of the ion

pair (the quadrupole formation) take place in a solution. The development of this analytical method has promoted our comprehension of the higher ion aggregation in solution.

ELUCIDATION OF SALT EFFECTS IN NONAQUEOUS SOLUTION ENVIRONMENTS

Salt effects on acid–base and metal indicators

Excluding a few anions in which the electric charges are delocalized symmetrically as ClO_4^- , many anions may have extraordinarily large interactions with alkali metal (M^+) and alkaline earth metal ions (M^{2+}) in protophobic aprotic solvents, possessing poor solvation abilities toward both anions and cations.

By the addition of MClO_4 and $\text{M}(\text{ClO}_4)_2$ to rhodamine B base (no HCl in this molecule), the intramolecule γ -lactone ring (C–O) was found to be cleaved within the MeCN solution. Only Mg^{2+} was effective for crystal violet lactone; the magnesium ion has strong interaction with the carboxylate ion from the lactone [49]. It has been concluded that the changes or developments in colors of acid–base sulfonephthalein indicators, such as phenol red and bromothymol blue, are caused by the γ -sultone-ring opening through the chemical interaction between the metal cations of added salts and the sulfonate ions from the sulfonephthalein indicators [50]. A practical fluoran-based black color former reacts with alkali metal and alkaline earth metal ions to develop the black color in MeCN [51].

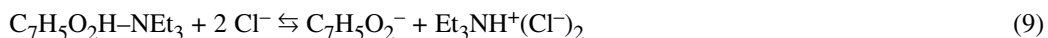
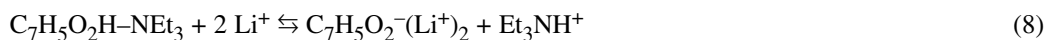
The Hammett acidity function, H_0 (corresponding to pH), with an acid–base indicator, “methyl yellow” [*p*-(dimethylamino)azobenzene], is changed by the addition of salts [52]; the salt effects have been explained by eq. 6, i.e., the ion-exchange reaction between the protonated indicator (Ind-H^+) and a large excess of metal ions and also by eq. 7, i.e., deprotonation from Ind-H^+ through the homoconjugation reaction; where X^- represents halide ions, Cl^- , Br^- , or I^- .



A metal indicator for the chelate titration, PAN [1-(2-pyridylazo)-2-naphthol], in aqueous solution, is regarded not to cause a distinct complex formation with alkaline earth metal ions. In MeCN, however, the distinct complex formation was observed between PAN and Mg^{2+} , accompanying the deprotonation from PAN. The interaction was also confirmed between Mg^{2+} and the diethylamino group in a derivative compound of PAN, 2-(5-bromo-2-pyridylazo)-5-diethylaminophenol [53].

“Contact ion pair” and “solvent-separated ion pair”

In MeCN [54], the proton-transfer reaction between tropolone ($\text{C}_7\text{H}_5\text{O}_2\text{H}$), a seven-member ring compound, and triethylamine (Et_3N) was much promoted by the addition of alkali metal and alkaline earth metal ions. On the other hand, the free tropolonate ion was produced by the addition of Et_4NCl to the equivalent mixture of tropolone-triethylamine (cf., eqs. 8 and 9). The absorption band of the tropolonate, combined with Li^+ , shifted toward shorter wavelengths than that of the free tropolonate ion.



The formation of dilithium tropolonate, $(\text{Li}^+)_2\text{L}^-$, and protonated tropolone, H_2L^+ , in acetonitrile was confirmed by ^1H and ^{13}C NMR data and theoretical calculations [55].

In the same solvent, the salt effects were examined on the proton transfer from various nitrophenols to bases; the addition of MClO_4 or $\text{M}(\text{ClO}_4)_2$ caused the formation of “contact ion pair” $[(\text{NO}_2)_2\text{C}_6\text{H}_3\text{O}^-(\text{M}^{2+})]$ (cf., Fig. 13) while Et_4NX ($\text{X} = \text{Cl}, \text{Br}$) produced the free phenolate ion $[(\text{Et}_4\text{N}^+) \cdots (\text{NO}_2)_2\text{C}_6\text{H}_4\text{O}^-]$ or “solvent-separated ion pair” (Fig. 14) [56].

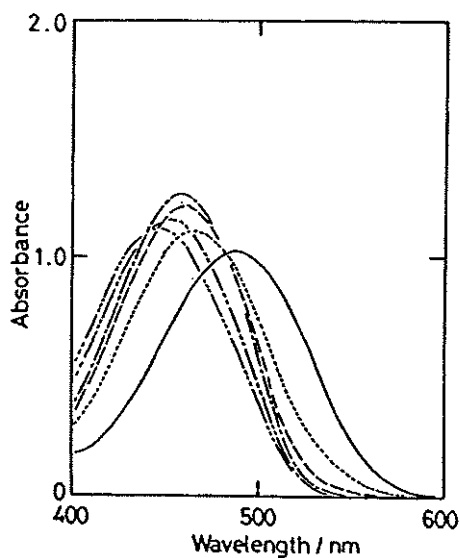


Fig. 13 Changes of visible absorption spectra of 2,5-dinitrophenolate ($[\text{Et}_4\text{N}^+ 2,5\text{-(NO}_2)_2\text{C}_6\text{H}_3\text{O}^-] = 2.0 \times 10^{-4} \text{ M}$) with increasing concentration of Li^+ in MeCN: (solid line) 0; (dotted line) 1.0×10^{-4} ; (broken line) 2.0×10^{-4} ; (solid line, single dot, solid line) 5.0×10^{-4} and 1.0×10^{-3} ; (solid line, double dot, solid line) 0.1; (solid line, triple dot, solid line) 0.2 M LiClO_4 .

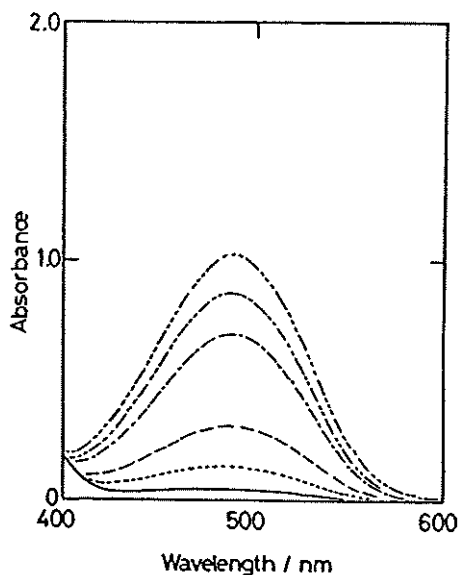


Fig. 14 Production of free 2,5-dinitrophenolate ions by the addition of various concentrations of Et_4NCl to $2.0 \times 10^{-4} \text{ M}$ 2,5-dinitrophenol + $2.0 \times 10^{-3} \text{ M}$ 2-chlorobenzylamine in MeCN: (solid line) 0; (dotted line) 1.0×10^{-3} ; (broken line) 1.0×10^{-2} ; (solid line, single dot, solid line) 0.1; (solid line, double dot, solid line) 0.2; (solid line, triple dot, solid line) 0.3 M Et_4NCl .

Concentrated salt effects on the solvolysis reaction rate

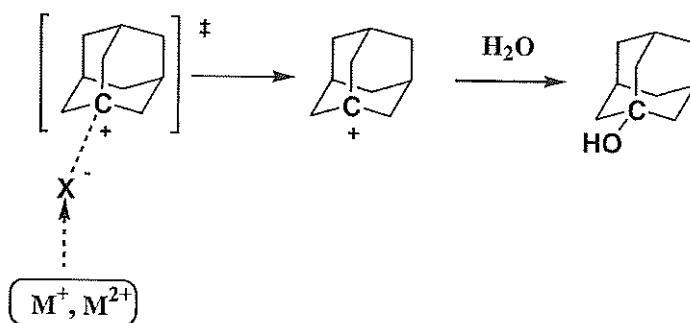
The stabilization of carbocations in solution is a matter of great interest in considering the mechanisms of organic reactions, especially S_N1 and S_N2 reactions in solvolysis. In some solvents, such as 1,2-dichloroethane and sulfur dioxide, triphenylmethyl chloride (trityl chloride, Ph_3CCl) can be ionized by itself. However, the ionization constant is too low to be estimated in MeCN. By the addition of metal chlorides, such as HgCl_2 , AlCl_3 , and SnCl_4 to Ph_3CCl solutions (MeCN and MeNO_2 solvents), the trityl cation (Ph_3C^+) can be formed even quantitatively through the following reaction [57]: $\text{Ph}_3\text{CCl} + \text{MCl}_m \rightleftharpoons \text{Ph}_3\text{C}^+ + [\text{MCl}_{m+1}]^-$.

By means of UV–vis absorption spectroscopy, we have found that the Ph_3C^+ ion is produced from Ph_3CX ($X = \text{Cl}, \text{Br}$) by the addition of MClO_4 ($M = \text{Li}, \text{Na}$) or $\text{M}(\text{ClO}_4)_2$ ($M = \text{Mg}, \text{Ca}, \text{Sr}, \text{Ba}$) in MeCN. The addition of the metal perchlorates to 4-MeO- substituted trityl chloride, $(4\text{-MeOC}_6\text{H}_4)_n\text{Ph}_{3-n}\text{CCl}$ ($n = 1\text{--}3$), caused the production of the corresponding trityl cations [49]; these reactions could be confirmed by ^1H and ^{13}C NMR chemical shifts [51,58], and were utilized for the preparation of trityl perchlorate compounds [58].

By the way, the addition of metal perchlorates, except for the Li^+ and Mg^{2+} salts, to trityl chlorides of relatively high concentrations caused the precipitation. We have confirmed that the precipitates by Ba^{2+} is not BaCl_2 but $\text{BaCl}^+\text{ClO}_4^-$ (the solubility of ca. 2.0×10^{-3} M in MeCN at 25 °C), based on the data of the chemical analysis, IR, X-ray diffraction, and TG-DTA [59].

It must be possible that a very small but direct “chemical” interaction between M^+ or M^{2+} and simple anions, such as halide and carboxylate ions, occurs even in aqueous or organic–aqueous solutions if they are in the “dihydrogen ether” conditions, as will be discussed in the following section. In kinetic studies, we have a merit to be able to amplify a minor increase in the concentration of an intermediate species, which can never be detected in the equilibrium sense, into an observable large increase in the reaction rate.

In MeOH– H_2O mixed solvent, the “pseudo” first-order reaction rates (k/s^{-1}) for typical S_N1 substrates, such as 1-adamantyl bromide and *t*-butyl chloride, were found to increase exponentially with increasing concentration of alkali metal or alkaline earth metal perchlorates, whereas with a nonmetallic salt (Et_4NBr), the reaction rates decreased [60]. The positive effects of Na^+ were smaller than those of Li^+ while the effects of Mg^{2+} or Ba^{2+} were much larger. We have concluded that the observed positive effects of the metal perchlorates are due to the formation of “stable” carbocations (R^+) through “chemical” interaction between the halides (X^-) and the metal cations (M^+, M^{2+}) in the “modified” solvent (cf. Scheme 4).



Scheme 4 The mechanism of enhanced solvolysis (hydrolysis) reaction of the S_N1 substrate in the presence of alkali metal (M^+) or alkaline earth metal ions (M^{2+}).

With the addition of the metal ions, the increase in the solvolysis rates was not observed for S_N1 – S_N2 intermediate substrates, isopropyl bromide and benzyl chloride. The addition of metal perchlorates to a S_N2 substrate, ethyl bromide, caused a decrease in the reaction rate. Similar results have been observed in acetone– H_2O [61], 1,2-dioxane– H_2O [62], MeCN– H_2O , DMF– H_2O [63], and sulfolane– H_2O [64] solvent systems.

Changes of water structure and formation of “dihydrogen ether”

According to Frank and Wen [65], the hydration of a salt causes the formation of three different regions around the ions as follows: A: region of immobilization of water molecules; B: region of structure breaking; and C: structurally “normal” water, i.e., the bulk water. The difference in the development of regions A and B determines whether an ion is of the structure-making or -breaking type. For instance, the Li^+ ion causes the development of A over B; therefore, Li^+ ion is classified as a structure-making ion. The development of region A by Cs^+ is small because of its weak hydration; Cs^+ is, therefore, a structure-breaking ion. This argument may be limited to low or moderate concentrations of a salt. However, we have proposed that the presence of highly concentrated salts in water or water-mixed solvents may cause the depression or disappearance of region C (of “ice-like-ness”) [60]. In such extreme conditions, only B (the broken-structure part) in the above model may be effective in the solvent function; the property of the aqueous solvent may be modified to be that of, as we term it, a “dihydrogen ether” $[R](H)-O-(H)[R]$ [62].

Figure 15 shows the Raman spectra of D_2O containing various concentrations of Et_4NBr at room temperature. The band at around 2510 cm^{-1} developed as the amount of water decreased ($R = [D_2O]/[salt]$) at the expense of the band at 2390 cm^{-1} . It has been reported that the Raman OD stretching spectrum of liquid D_2O spans from ca. 2000 to 2800 cm^{-1} with a peak wavenumber of ca. 2510 cm^{-1} [66]. Scherer et al. [67] have reported Raman spectra of liquid D_2O from -10 to $90\text{ }^\circ\text{C}$; the (isotropic) spectra show the development of a band around 2500 cm^{-1} at the expense of the band around 2400 cm^{-1} with increasing temperature. These bands have been attributed to the OD stretching vibration of the symmetrically hydrogen-bonded complexes (2400 cm^{-1}) and of the single-handed complex (2500 cm^{-1}). At any rate, the (partial) breaking or cleavage of hydrogen bond of liquid D_2O with increasing temperature caused the development of the band around 2500 cm^{-1} . Therefore, the spectrum changes caused by increasing concentration of Et_4NBr can be attributed to the cleavage of hydrogen

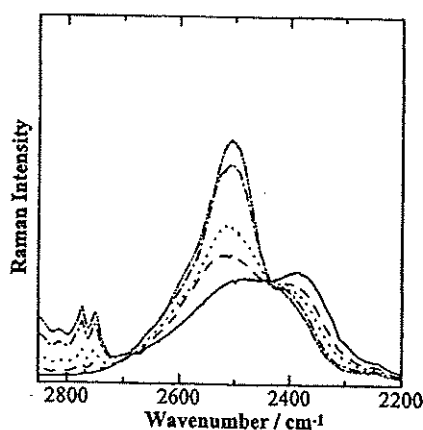


Fig. 15 The Raman spectra of D_2O containing various amounts of Et_4NBr at room temperature: (solid line) no salt; (broken line) $R = 20$; (dotted line) $R = 10$; (solid line, single dot, solid line) $R = 5$; (solid line, double dot, solid line) $R = 3.75$ where $R = [D_2O]/[Et_4NBr]$.

bonding; that is, the large clusters of D₂O are destroyed and turned into smaller clusters by the addition of the highly concentrated salt.

Brink and Falk [68] have reported the OD stretching band (in IR spectra) of HDO in aqueous solutions of NaClO₄ and Mg(ClO₄)₂ of varying concentrations at 28 °C. A band at 2500 cm⁻¹ (OD stretching of hydrogen-bonded HDO) in the absence of the salts was overtaken by a high-frequency band (ca. 2620–2630 cm⁻¹) with increasing concentration of the salts. Regarding their observations, Varrall [69] has commented that the high-frequency component is due to the extensive breakdown of hydrogen-bonded water structure by ClO₄⁻, an effect similar to that of increasing temperature.

Tetraalkylammonium (R₄N⁺) salts are usually regarded as having structure-making properties, based on their “hydrophobic effect”, larger than expected from their cationic sizes. However, in 20 vol % EtOH–H₂O, the proton NMR chemical shift suggested that the R₄N⁺ ions have the tendency to destroy the water structure; the longer the alkyl chain, the highly being destroyed [70]. At any rate, Et₄NBr appears to be one of the most suitable salts for observing the vibration spectra of the solvent part (regions B and C) and not the hydration part (region A), since neither the Et₄N⁺ nor Br⁻ are strongly hydrates in aqueous solutions and also their solubility in water is very high at room temperature. Verrall [69] also has mentioned that the R₄NBr series appears to offer a better basis for rationalizing purely structural effects. While admitting that D₂O is a more structured liquid than H₂O [71], we feel that the whole argument for D₂O could basically be applied to H₂O and H₂O-mixed solvents. In addition, the Raman spectra of D₂O with concentrated LiBr showed great increases in the intensity around 2530 cm⁻¹ at the expense of the band at ca. 2390 cm⁻¹ [72].

The water structure is found to be distorted in D₂O-containing organic solvents, such as DMF and sulfolane; the addition of Et₄NBr or LiClO₄ to the D₂O-organic solvent mixture caused further distortion of water structure [63,64]. Thus, it seems that the authentic properties of bulk water may be modified to be those of “dihydrogen ether” or they may approach the properties of a “nonaqueous solvent” with increasing content of organic solvents or salts.

It has been clearly demonstrated that the small water droplets (nm-size) in organic solvents, i.e., in reverse micelle systems, should lose further their properties as water with the addition of salts [72]. By the addition of LiClO₄, the color of CoCl₂ or CoBr₂ was altered from pale red (or almost no color) to deep blue in the water droplets in chloroform reverse micelle systems with cetyltrimethylammonium chloride or bromide as the surfactant, [CHCl₃/CTAC (or CTAB)/H₂O (1.0 vol %)]. The increase of blue color indicated the formation of the [CoX₄]²⁻ complexes, which suggested that the complexes exist in a dry condition and not a wet one. Bjerrum et al. [73] reported the overall formation constant, β₄ = [CoCl₄²⁻]/[Co²⁺][Cl⁻]⁴ in aqueous solution to be 10^{-6.6} and 10⁴ at the ionic strength of zero and 9 M HClO₄ media, respectively. The great increase in the formation constant with the addition of 9 M HClO₄, as high as a 1.5 × 10¹⁰-fold, has been attributed to the “increase” in activity coefficients of ions up to γ_± ~ 350. By the way, we have observed a great enhancement in the oxidation ability of dilute HNO₃ in nanoscale water droplets of reverse micelle systems [74]; the phenomena may not be explained by the change in activity coefficients of ions. Recently, Crans et al. [75] suggested that some properties of the water inside the reverse micelle even with *w* > 10 (*w* = [H₂O]/[surfactant]) are different from those of the bulk water.

Postorino et al. reported that no hydrogen-bonding structure of water existed in supercritical water conditions [76]. However, it must be natural that the hydrogen-bonding structure remains, to some extent, in the rather condensed phase of the supercritical water, as water molecule aggregation can be formed even in the vapor phase [5]. Anyway, it may be true that the hydrogen-bonding structure in supercritical water is remarkably destroyed and the properties of water are almost lost. The higher ion aggregates from NaCl in supercritical water conditions have been suggested [77].

We would like to note that the properties of bulk water should disappear in the conditions that a huge network of water cannot be constructed, since water may gain the bulk water properties upon the formation of the huge network of water molecules. In the following cases, water may lose the authentic properties, more or less, as the bulk water: (a) the residual water (~ mM) in organic solvents; (b)

aqueous solutions or organic solvent–water mixtures containing highly concentrated salts; (c) nanosize water droplets in nanotube or reverse micellar systems (the number of water, $n_w < \sim 10^7$); (d) waters on metal electrodes, ion-exchange resins, proteins, organic solvents as the solvent extraction, and glass vessels; (e) the water in supercritical conditions. Such waters may be “reduced” into the authentic H_2O molecules (as the “dihydrogen ether,” $[R](H)-O-(H)[R]$).

CONCLUDING REMARKS

The studies mentioned above have been performed based on the idea that alkali metal or alkaline earth metal ions have potentially “coordination” abilities, as strongly as to involve directly in chemical reactions, although such metal ions have been regarded to possess almost no chemical reactivity in solution. Thus, a comprehensive framework may be given for the extraordinary deviations in chemical equilibria and kinetics in solutions containing concentrated salts, which cannot be dealt with by the conventional idea without some contradiction.

Even though it is admitted that such “chemical” interactions may be observed without difficulty in poor solvating media, the interactions may never be observed directly in aqueous solution since the reactive moieties in anions or cations are already shielded by the strong acidity or basicity of water. As the practical science, now, we are able to supply the interaction between alkali metal ions and many anions through adopting an alternative procedure that minor changes in chemical equilibria are accumulated for every second, i.e., the translation of indeterminable concentration changes in chemical equilibria into observable changes in chemical reaction rates.

We dare to describe that the role of a transition-metal ion (e.g., Cd^{2+}) in aqueous solution can be played by an alkaline earth metal ion (e.g., Ca^{2+}) in nonaqueous solution. A similar relationship may stand between H^+ in aqueous solution and Li^+ in nonaqueous (protophobic aprotic) solvents. However, one may guess still that some chemists cannot accept the idea that alkali metal ions are directly involved in chemical reactions in solution, reflecting the “common” recognition for the metal ions in solution.

It has been shown, in the present paper, that comprehensive interpretations without contradiction are turned to be possible in many systems by taking account of the chemical bonding force of alkali metal or alkaline earth metal ions in solution.

The present paper is based on the contents of account articles in Japanese [M. Hojo. *Bunseki Kagaku* **53**, 1279 (2004)] and in English [M. Hojo. *Kharkov Univer. Bull.*, No. 626, Chemical Series, Issue 11(34), 47–64 (2004)].

REFERENCES

1. N. O. Mchedlov-Petrossyan, V. I. Kukhtik, V. D. Bezugliy. *J. Phys. Org. Chem.* **16**, 380 (2003).
2. J. F. Coetzee, I. M. Kolthoff. *J. Am. Chem. Soc.* **79**, 6110 (1957).
3. M. Kinugasa, K. Kishi, S. Ikeda. *J. Phys. Chem.* **77**, 1914 (1973).
4. C. K. Mann. In *Electroanalytical Chemistry*, Vol. 3, A. J. Bard (Ed.), p. 69, Marcel Dekker, New York (1969).
5. K. Liu, J. D. Cruzan, R. J. Saykally. *Science* **271**, 929 (1996).
6. V. Gutmann. *The Donor-Acceptor Approach to Molecular Interactions*, p. 21, Plenum, New York (1978).
7. W. J. Moore. *Basic Physical Chemistry*, Chap. 6, Prentice-Hall, Englewood Cliffs (1983).
8. R. M. Silverstein, G. C. Bassler, T. C. Morill. *Spectrometric Identification of Organic Compounds*, 5th ed., Chap. 4, John Wiley, New York (1991).
9. D. R. Cogley, M. Falk, J. N. Butler, E. Grunwald. *J. Phys. Chem.* **76**, 855 (1972).
10. K. Mizuno, S. Imafuji, T. Ochi, T. Ohta, S. Maeda. *J. Phys. Chem. B* **104**, 11001 (2000).
11. M. Hojo, Z. Chen. *Anal. Sci.* **15**, 303 (1999).
12. I. M. Kolthoff, M. K. Chantooni Jr. *J. Am. Chem. Soc.* **85**, 426 (1963).

13. M. Hojo, H. Hasegawa, Z. Chen. *Bull. Chem. Soc. Jpn.* **69**, 2215 (1996).
14. P. G. Daniele, C. Rigano, S. Sammartano. *Anal. Chem.* **57**, 2956 (1985).
15. A. De Robertis, C. De Stefano, C. Rigano, S. Sammartano, R. Scarcella. *J. Chem. Res. (S)* **42** (1985).
16. R. M. Izatt, K. Pawlak, J. S. Bradshaw. *Chem. Rev.* **91**, 1721 (1991).
17. M. Hojo, M. Hagiwara, H. Nagai, Y. Imai. *J. Electroanal. Chem.* **234**, 251 (1987).
18. M. Hojo, H. Hasegawa, T. Ohno, S. Arisawa, K. Chayama. *Anal. Sci.* **11**, 419 (1995).
19. M. Hojo, I. Hisatsune, H. Tsurui, S. Minami. *Anal. Sci.* **16**, 1277 (2000).
20. M. Hojo, Y. Imai. *J. Electroanal. Chem.* **209**, 297 (1986).
21. M. Hojo, Y. Imai. *Bull. Chem. Soc. Jpn.* **56**, 1963 (1983).
22. M. Hojo, T. Takiguchi, M. Hagiwara, H. Nagai, Y. Imai. *J. Phys. Chem.* **93**, 955 (1989).
23. M. Hojo, H. Hasegawa, Y. Miyauchi, H. Moriyama, H. Yoneda, S. Arisawa. *Electrochim. Acta* **39**, 629 (1994).
24. R. W. Murray, L. K. Hiller Jr. *Anal. Chem.* **39**, 1221 (1967).
25. E. Itabashi. *J. Electroanal. Chem.* **36**, 179 (1972).
26. M. Hojo, A. Tanio, Y. Miyauchi, Y. Imai. *Chem. Lett.* 1827 (1991).
27. M. Hojo, Y. Miyauchi, N. Ide, A. Tanio, Y. Imai. *J. Electroanal. Chem.* **340**, 197 (1992).
28. F. Klanberg, J. P. Hunt, H. W. Dodgen. *Inorg. Chem.* **2**, 139 (1963).
29. J. E. Hickey, M. S. Spritzer, P. J. Elving. *Anal. Chim. Acta* **35**, 277 (1966).
30. M. Hojo, Y. Akita, K. Nishikawa, Y. Imai. *Bull. Chem. Soc. Jpn.* **60**, 509 (1987).
31. K. Tsuji, P. J. Elving. *Anal. Chem.* **41**, 1571 (1969).
32. R. M. Fuoss, C. A. Kraus. *J. Am. Chem. Soc.* **55**, 2389 (1933).
33. B. Gestblom, I. Svorstol, J. Songstad. *J. Phys. Chem.* **90**, 4684 (1986).
34. S. Petrucci, E. M. Eyring. *J. Phys. Chem.* **95**, 1731 (1991).
35. Z. Chen, M. Hojo. *J. Phys. Chem. B* **101**, 10896 (1997).
36. R. M. Fuoss, F. Accascina. *Electrolytic Conductance*, p. 256, Interscience, New York (1959).
37. M. Hojo, T. Ueda, Z. Chen, M. Nishimura. *J. Electroanal. Chem.* **468**, 110 (1999).
38. Y. Miyauchi, M. Hojo, N. Ide, Y. Imai. *J. Chem. Soc., Faraday Trans.* **88**, 1425 (1992).
39. Y. Miyauchi, M. Hojo, H. Moriyama, Y. Imai. *J. Chem. Soc., Faraday Trans.* **88**, 3175 (1992).
40. T. Shedlovsky. *J. Franklin Inst.* **225**, 739 (1938).
41. Y. Wu, H. L. Friedman. *J. Phys. Chem.* **70**, 501 (1966).
42. M. L. Jansen, H. L. Yeager. *J. Phys. Chem.* **78**, 1380 (1974).
43. J. Barthel, H.-J. Gores, L. Kraml. *J. Phys. Chem.* **100**, 3671 (1996).
44. M. Hojo, T. Ueda, M. Nishimura, H. Hamada, M. Matsui, S. Umetani. *J. Phys. Chem. B* **103**, 8965 (1999).
45. G. Ruderman, E. R. Caffarena, I. G. Mogilner, E. J. Tolosa. *J. Solution Chem.* **27**, 935 (1998).
46. K. Suzuki, Y. Taniguchi, T. Watanabe. *J. Phys. Chem.* **77**, 1918 (1973).
47. A. Katchalsky, H. Eisenberg, S. Lifson. *J. Am. Chem. Soc.* **73**, 5889 (1951).
48. D. A. MacInnes, T. Shedlovsky. *J. Am. Chem. Soc.* **54**, 1429 (1932).
49. M. Hojo, H. Hasegawa, H. Tsurui, K. Kawamura, S. Minami, A. Mizobe. *Bull. Chem. Soc. Jpn.* **71**, 1619 (1998).
50. M. Hojo, T. Ueda, K. Kawamura, M. Yamasaki. *Bull. Chem. Soc. Jpn.* **73**, 347 (2000).
51. M. Hojo, T. Ueda, M. Yamasaki, A. Inoue, S. Tokita, M. Yanagita. *Bull. Chem. Soc. Jpn.* **75**, 1569 (2002).
52. M. Hojo, H. Hasegawa, H. Yoneda. *Bull. Chem. Soc. Jpn.* **69**, 971 (1996).
53. M. Hojo, T. Ueda, A. Inoue. *Bull. Chem. Soc. Jpn.* **75**, 2629 (2002).
54. M. Hojo, H. Hasegawa, H. Yoneda. *J. Chem. Soc., Perkin Trans. 2* 1855 (1994).
55. M. Hojo, T. Ueda, T. Inoue, M. Ike, M. Kobayashi, H. Nakai. *J. Phys. Chem. B* **111**, 1759 (2007).
56. M. Hojo, H. Hasegawa, A. Mizobe, Y. Ohkawa, Y. Miimi. *J. Phys. Chem.* **99**, 16609 (1995).
57. M. Baaz, V. Gutmann, O. Kune. *Monatsh. Chem.* **93**, 1142 (1962).

58. M. Hojo, T. Ueda, M. Yamasaki. *J. Org. Chem.* **64**, 4939 (1999).
59. M. Hojo, T. Ueda, M. Yamasaki, A. Inoue. *Anal. Sci.* **16**, 649 (2000).
60. L. C. Manege, T. Ueda, M. Hojo. *Bull. Chem. Soc. Jpn.* **71**, 589 (1998).
61. L. C. Manege, T. Ueda, M. Hojo, M. Fijio. *J. Chem. Soc., Perkin Trans. 2* 1961 (1998).
62. M. Hojo, T. Ueda, S. Inoue, Y. Kawahara. *J. Chem. Soc., Perkin Trans. 2* 1735 (2000).
63. M. Hojo, E. Ueno. Unpublished data.
64. M. Hojo, T. Ueda, E. Ueno, T. Hamasaki, D. Fujimura. *Bull. Chem. Soc. Jpn.* **79**, 751 (2006).
65. H. S. Frank, W.-Y. Wen. *Discuss. Faraday Soc.* **24**, 133 (1957).
66. Y. Yoshimura, H. Kanno. *J. Raman Spectrosc.* **27**, 671 (1996).
67. J. R. Scherer, M. K. Go, S. Kint. *J. Phys. Chem.* **78**, 1304 (1974).
68. G. Brink, M. Falk. *Can. J. Chem.* **48**, 3019 (1970).
69. R. E. Verrall. In *Water, A Comprehensive Treatise*, Vol. 3, F. Franks (Ed.), Chap. 5, Plenum, New York (1973).
70. A. Nose, M. Hojo, T. Ueda. *J. Phys. Chem. B* **108**, 798 (2004).
71. J. E. Gordon. *The Organic Chemistry of Electrolytes Solutions*, p. 167, John Wiley, New York (1975).
72. H. Nagayama, M. Hojo, T. Ueda, Y. Nishimori, M. Okamura, C. Daike. *Anal. Sci.* **17**, 1413 (2001).
73. J. Bjerrum, A. S. Halonin, L. H. Skibsted. *Acta Chem. Scand. A* **29**, 326 (1975).
74. M. Hojo, T. Ueda, C. Daike, F. Takezaki, Y. Furuya, K. Miyamoto, A. Narutaki, R. Kato. *Bull. Chem. Soc. Jpn.* **79**, 1215 (2006).
75. B. Baruah, J. M. Roden, M. Sedgwick, N. M. Correa, D. C. Crans, N. E. Levinger. *J. Am. Chem. Soc.* **128**, 12758 (2006).
76. P. Postorino, R. H. Tromp, M.-A. Ricci, A. K. Soper, G. W. Neilson. *Nature* **366**, 668 (1993).
77. E. H. Oelkers, H. C. Helgeson. *Science* **261**, 888 (1993).